STEM CELLS AND DEVELOPMENT
Volume 31, Numbers 7–8, 2022

DOI: 10.1089/scd.2021.0316

Downregulating *MFN2* Promotes the Differentiation of Induced Pluripotent Stem Cells into Mesenchymal Stem Cells through the PI3K/Akt/GSK-3β/Wnt Signaling Pathway

Lidi Deng,[1] Siqi Yi,[1] Xiaohui Yin,[2] Yang Li,[3] and Qingxian Luan[1]

Understanding the mechanism of the differentiation of induced pluripotent stem cells (iPSCs) into mesenchymal stem cells (MSCs) and promoting the production efficiency of iPSC-derived MSCs (iPSC-MSCs) are critical to periodontal tissue engineering. However, the gene networks that control this differentiation process from iPSCs into MSCs are poorly understood. We demonstrated that *MFN2* knockdown showed a positive effect on the triploblastic and MSC differentiation from iPSCs. Activation of the PI3K/Akt signaling pathway by *MFN2* knockdown activated the Wnt/β-catenin signaling pathway by inhibiting GSK-3β and reducing β-catenin degradation. Inhibitor of the PI3K/Akt signaling pathway normalized the enhanced efficiency of differentiation into MSCs of *MFN2*-KD iPSCs and Wnt activator-treated control iPSCs. *MFN2*-OE iPSCs displayed an opposite phenotype. In conclusion, downregulating *MFN2* promotes the differentiation of iPSCs into MSCs by activating the PI3K/Akt/GSK-3β/Wnt signaling pathway. Our results reveal a crucial function and mechanism for *MFN2* in regulating MSC differentiation from iPSCs, which will provide new ideas for periodontal tissue engineering and periodontal regenerative treatment by using iPSC-MSCs.

Keywords: *MFN2*, induced pluripotent stem cells, mesenchymal stem cells, differentiation, PI3K/Akt signaling pathway, Wnt/β-catenin signaling pathway

Introduction

Currently, periodontal tissue engineering mainly applies mesenchymal stem cells (MSCs) derived from autologous tissues, such as bone marrow, fat tissue, and periodontal ligament [1]. MSCs are adult stem cells derived from mesoderm that can produce a variety of specialized cell types, but the number of MSCs derived from these tissues is limited. Pluripotent stem cells (PSCs), including embryonic stem cells (ESCs) and induced pluripotent stem cells (iPSCs), alleviate this problem to a certain extent. These cells have unlimited self-renewal capacity and can produce almost all cells derived from endoderm, mesoderm, and ectoderm [2,3]. Therefore, theoretically, iPSC-derived MSCs (iPSC-MSCs) can be obtained indefinitely, which are phenotypically stable and safe concerning tumor formation [4].

Current studies report that iPSCs generated from one tissue have a greater capacity to form cells from the original tissue [5,6]. This finding provides a good rationale for using periodontal tissue-derived iPSCs for periodontal regeneration. Our previous work reported that iPSCs can be established from gingival fibroblasts of dental tissue origin [7]. Previous studies showed that MSCs can be differentiated from PSCs [8], but a more time-saving method is needed.

Mitochondria are important organelles to synthesize ATP, and critical for maintaining normal physiological functions such as cell metabolism, cell differentiation, cell

Departments of [1]Periodontology and [2]First Clinical Division, Peking University School and Hospital of Stomatology & National Center of Stomatology & National Clinical Research Center for Oral Diseases & National Engineering Laboratory for Digital and Material Technology of Stomatology & Beijing Key Laboratory of Digital Stomatology & Research Center of Engineering and Technology for Computerized Dentistry Ministry of Health & NMPA Key Laboratory for Dental Materials, Beijing, People's Republic of China.
[3]Department of Cell Biology, School of Basic Medical Sciences, Peking University Stem Cell Research Center, Peking University, Beijing, People's Republic of China.

cycle, and biosynthesis. Mitochondria continuously change their shape through fusion and fission to respond to different needs [9]. The morphological changes of mitochondria are mainly controlled by a series of GTPases that participate in the regulation of mitochondrial fusion and fission. Mitofusin-1 (*MFN1*), mitofusin-2 (*MFN2*), and optic atrophy-1 (*OPA1*) are involved in mitochondrial fusion [10].

MFN2 is critical in the process of embryonic development, and its knockout leads to the death of mouse embryos [11]. Studies have shown that knockdown of *MFN2* led to defects in mitochondrial metabolism, neurogenesis, and synapse formation. Overexpressing *MFN2* enhanced the biological energy and function of mitochondria and promoted the differentiation and maturation of iPSC-derived cortical neurons [12]. Lack of mitofusin affects mouse spermatogonial differentiation and the formation of spermatocytes [13].

It has been reported that PI3K/Akt signaling pathway is closely related to *MFN2* [14]. GSK3β is one of the downstream targets of the PI3K/Akt signaling pathway. Inhibition of GSK3β through activating the PI3K/Akt signaling pathway stabilizes and translocates β-catenin into the nucleus for gene transcription [15]. Previous studies have shown that the phosphorylation of AKT inhibits the activity of GSK3β, thereby activating the downstream Wnt/β-catenin signaling pathway and promoting mesoderm differentiation of PSCs [16]. The Wnt/β-catenin pathway plays an important role in the development of many mesoderm-derived tissues and organs [17]. However, the roles and interrelationships of *MFN2*, PI3K/Akt, and Wnt/β-catenin signaling pathways in the differentiation of iPSCs into MSCs have not been studied yet.

In this study, we raised the hypothesis that *MFN2* participated in MSC differentiation from iPSCs. To address the specific roles of *MFN2* during MSC differentiation from human iPSCs, we generated *MFN2* knockdown (*MFN2*-KD) and *MFN2* overexpressing (*MFN2*-OE) iPSCs derived from human gingival fibroblasts, which were induced toward MSCs in vitro. Our data showed that the knockdown of *MFN2* in iPSCs promoted the differentiation capacity to MSCs. Conversely, *MFN2*-OE iPSCs displayed an opposite phenotype. Lastly, we demonstrated that knockdown of *MFN2* promoted the differentiation of iPSCs into MSCs by activating the PI3K/Akt/GSK-3β/Wnt signaling pathway. This study reveals a crucial function and mechanism for *MFN2* in regulating MSC differentiation from iPSCs.

Materials and Methods

Cell culture

iPSCs were reprogrammed from human gingival fibroblasts in our previous studies [7], which are derived from wasted human gingival tissues from third molar removal surgery or orthodontic therapy with informed consent. The protocols were approved by the Biomedical Ethics Committee, Peking University Hospital of Stomatology (No. PKUSSIRB-201414048). The iPSCs were expanded and passaged in TeSR-E8 medium (Stemcell Technologies) and Matrigel (Corning) precoated culture plates. All cells were cultured in a cell culture incubator (Thermo Fisher Scientific) containing 5% CO_2 at 37°C.

Construction of MFN2-KD iPSCs by lentivirus

The siRNA target gene sequence for *MFN2* was designed according to the RNAi sequence design principles. The sequence was GGAAGAGCACCGTGATCAATG. The virus vector framework was constructed, the plasmid transformation was conducted, and the transformed *E. coli* was screened by ampicillin-containing agar plate. We identified and sequenced the PCR product, and extracted the *E. coli* solution with the correct sequencing result. Then, we added pGag/Pol, pRev, and pVSV-G to package the lentiviral particles and infected the 293T cells, and concentrated the virus in an ultracentrifuge (Beckman Coulter). For infection, fresh TeSR-E8 medium containing concentrated virus was added to the iPSCs, and the positive iPSCs were screened with puromycin (Thermo Fisher Scientific) 48 h after infection.

Construction of MFN2-OE iPSCs by lentivirus

The linearized GV492 vector (Genechem) was obtained by digestion with restriction enzymes *Bam*HI and *Age*I. The target gene fragment (NM_014874, 2274 bp) was amplified by PCR using primers with homologous recombination sequence (underlined) added to the 5'end (Primers: *MFN2*–1: AGGTCGACTCTAGAGGATCCCGCCACCATGTCCCTGCTCTTCTCTCG; and *MFN2*–2: TCCTTGTAGTCCATACCTCTGCTGGGCTGCAGGTACTGGTG). The linearized vector and target gene fragment were connected by a homologous recombination reaction. The following steps, such as transformation, virus packaging, purification, and infection, were the same as the construction of *MFN2*-KD iPSCs.

Western blot analysis

The cells were lysed in RIPA lysis and Extraction buffer (Thermo Fisher Scientific). All proteins were separated by SDS-PAGE electrophoresis and transferred to polyvinylidene difluoride membrane (Merck Millipore). The blot was incubated by primary and secondary antibodies after blocking in 5% defatted milk. Immobilon ECL Ultra Western HRP substrate (Merck Millipore) was applied to visualize the protein band. The antibodies were as follows: MFN2 (1:1,000; Abcam), GAPDH (1:1,000; CST), RUNX2 (1:1,000; Proteintech), OSX (1:1,000; Abcam), AKT (1:1,000; Proteintech), phosphor-AKT (pAKT, 1:1,000; Proteintech), pGSK-3β (1:1,000; CST), GSK-3β (1:1,000; CST), VDAC (1:1,000; Proteintech), and β-catenin (1:1,000; Proteintech).

Quantitative real-time polymerase chain reaction analysis

TRIzol reagent (Thermo Fisher Scientific) was added to the cell samples to extract total RNA. According to the manufacturer's instructions, reverse transcription was performed with the PrimeScript RT Kit (TaKaRa, Japan) to obtain cDNA. Quantitative real-time polymerase chain reaction (qRT-PCR) was performed by Power Up SYBR Green master mix (Thermo Fisher Scientific) in CFX384 Touch Real-Time PCR Detection System (Bio-Rad). The primer sequences are shown in Table 1; *ACTB* was employed as an internal control.

Table 1. Primer Sequences Used for Quantitative Real-Time Polymerase Chain Reaction

Gene	*Forward primer (5′–3′)*	*Reverse primer (5′–3′)*
MFN2	CACAAGGTGAGTGAGCGTCT	CGTTGAGCACCTCCTTAGCA
PAX6	CGAGACTGGCTCCATCAGAC	CTTTTCGCTAGCCAGGTTGC
SOX1	CAACCAGGACCGGGTCAAAC	CCTCGGACATGACCTTCCACT
T	TATGAGCCTCGAATCCACATAGT	CCTCGTTCTGATAAGCAGTCAC
MESP1	TCGAAGTGGTTCCTTGG	TGCTTGCCTCAAAGTGTC
SOX17	CCTTCACGTGTACTACGGCG	GTTCAAATTCCGTGCGGTCC
GATA4	CTGGCCTGTCATCTCACTACG	GGTCCGTGCAGGAATTTGAGG
COX7A1	GGAACCGCTTTCAGAACCGA	CACAGCGTCATTGTCACTCG
NDUFB6	TCCATGGGGTATACAAAAAGAG	GGAAATTCTTTCATTGGTGGA
NT5E (CD73)	GGGCGGAAGGTTCCTGTAG	GAGGAGCCATCCAGATAGACA
ENG (CD105)	AGCCCCACAAGTCTTGCAG	GCTAGTGGTATATGTCACCTCGC
RUNX2	TCTAAATCGCCAGGCTTCAT	GAGGACCTACTCCCAAAGGA
OSX	TCCCTGCTTGAGGAGGAAG	TAGCATAGCCTGAGGTGGGT
PPARG	TCTGGCCCACCAACTTTGGG	CTTCACAAGCATGAACTCCA
SOX9	GGCAAGCTCTGGAGACTTCTG	CCCGTTCTTCACCGACTTCC
ACTB	CTCGCCTTTGCCGATCC	TCTCCATGTCGTCCCAGTTG

Immunofluorescence

The cells were fixed in 4% paraformaldehyde solution for 30 min, gently rinsed three times with phosphate-buffered saline (PBS), permeabilized in 0.3% Triton X-100 (Sigma-Aldrich) in PBS for 20 min, and blocked with 5% bovine serum albumin (BSA) (Sigma-Aldrich) in PBS for 1 h at room temperature. The cells were stained by primary antibody MFN2 (1:100; Abcam) at room temperature for 1 h, then incubated by secondary antibody DyLight 488 (ZSGB-Bio) for 1 h. The nucleus was stained by DAPI (Thermo Fisher Scientific). Images were observed and recorded by a confocal microscope (Leica).

Flow cytometry

The cells were digested with Accutase (Merck Millipore) and stained with antibody for 30 min in the dark at 4°C. The cells were then washed twice with PBS, resuspended in PBS, and analyzed by CytoFLEX S flow cytometer (Beckman Coulter) and Cytexpert software (ver. 2.3; Beckman Coulter). The antibodies were as follows: CD34-PE (BD Biosciences), CD45-APC-A750 (eBioscience), CD73-FITC (eBioscience), CD90-FITC (BioLegend), and CD146-PE (BioLegend).

Three germ layer differentiation of iPSCs

Neural ectoderm, hematopoietic progenitor cell (mesoderm), and endoderm differentiation were performed according to the protocols described in our previous study [18]. qRT-PCR and flow cytometry analyses were carried out 3 days after differentiation.

Extracellular oxygen consumption assay

Cells were seeded on a 96-well plate. The relative oxidative phosphorylation (basal and maximal respiration) rate was measured by fluorescence intensity in a fluorescence microplate reader (Molecular Devices) with the Mitochondrial Stress Test Complete Assay Kit (Abcam) according to the manufacturer's protocols. Basal respiration rate represents the cellular energy requirements under basal conditions. Maximal respiration rate refers to the cellular maximum respiration potential treated with FCCP.

Derivation and multilineage differentiation of iPSC-MSCs

According to the manufacturer's instructions, on day 1–3, the TeSR-E8 medium was replaced by 3 mL STEMdiff™-ACF mesenchymal induction medium (Stemcell Technologies). On day 4–5, the medium was replaced by 2 mL MesenCult™-ACF Plus medium (Stemcell Technologies). On day 6, the cells were passaged and cultured with MesenCult-ACF Plus medium. Flow cytometry and total RNA extraction were performed on day 8. On day 6 to day 21, cells were passaged at ~80% confluence and cultured with MesenCult-ACF Plus medium.

Multilineage differentiation was performed on day 21. For the osteogenic differentiation of iPSC-MSCs, the medium was replaced by DMEM supplemented with 10% FBS (Gibco), 10 mM sodium β-glycerophosphate, 50 μM vitamin C, and 0.1 μM dexamethasone (Sigma-Aldrich). Alizarin Red staining was performed on day 42.

For adipogenic differentiation, the medium was replaced by DMEM supplemented with 10% FBS, 10 μM insulin, 200 μM indomethacin, 0.5 μM IBMX (Sigma-Aldrich), and 1 μM dexamethasone. Oil Red O staining was performed on day 42. For chondrogenic differentiation, the medium was replaced by DMEM supplemented with 10% FBS, 100 μg/mL sodium pyruvate, 40 μg/mL proline (Sigma-Aldrich), 50 μg/mL vitamin C, 10 ng/mL TGF-β1 (R&D Systems), and 0.1 μM dexamethasone. Alcian Blue staining was performed on day 42. Multilineage differentiation markers, *RUNX2*, *PPARG*, and *SOX9*, were detected accordingly by qRT-PCR on day 42. The timeline of the differentiation and induction process was summarized in Supplementary Fig. S1.

RNA-sequencing

One microgram total RNA of the control and *MFN2*-KD iPSCs was collected and processed by the NEBNext Ultra RNA Library Prep Kit for Illumina (NEB) to generate a

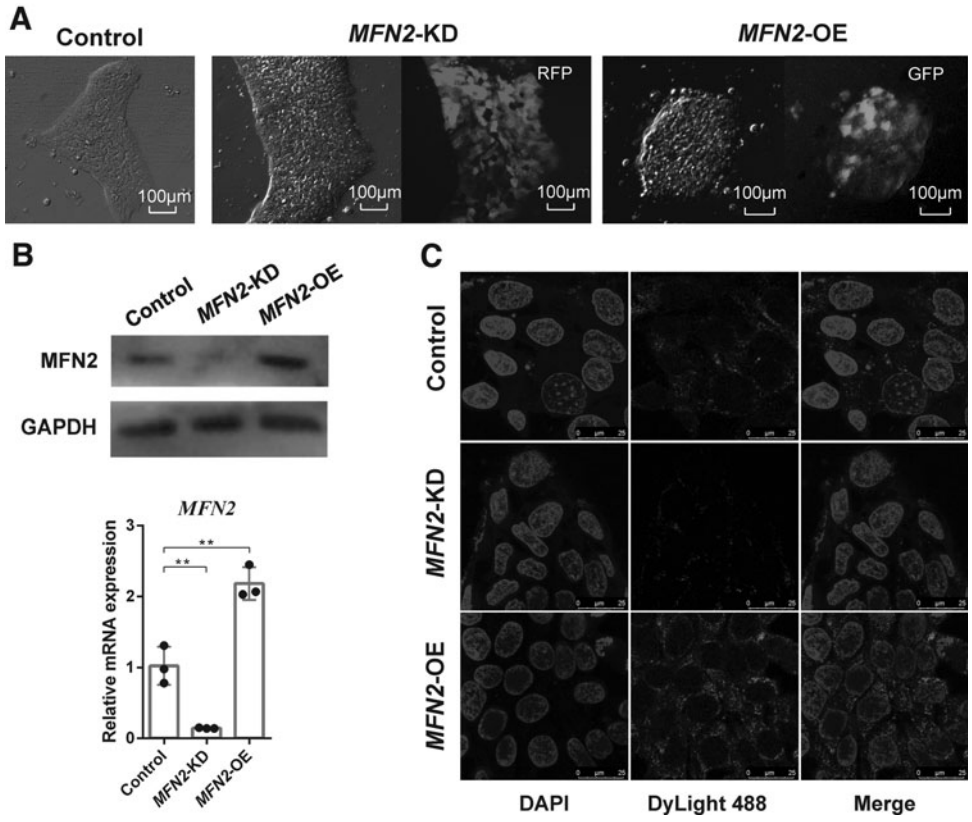

FIG. 1. Construction and identification of *MFN2*-KD and *MFN2*-OE iPSCs. **(A)** The morphology of control, *MFN2*-KD, and *MFN2*-OE iPSCs under optical and fluorescence microscope. Western blot, qRT-PCR **(B)** and immunofluorescence **(C)** analysis of MFN2 in control, *MFN2*-KD, and *MFN2*-OE iPSCs. *MFN2*-KD, *MFN2* knockdown. *MFN2*-OE, *MFN2* overexpressing. Data are expressed as mean ± SD, $^{**}P < 0.01$. qRT-PCR, quantitative real-time polymerase chain reaction; iPSC, induced pluripotent stem cell.

sequencing library. The library preparations were sequenced on the Illumina platform. Differential expression analysis was performed on DESeq2 R software, and genes with a *P* value <0.05 were considered differentially expressed. Kyoto Encyclopedia of Genes and Genomes (KEGG) pathway and Gene Ontology (GO) enrichment analysis on differentially expressed genes, and gene set enrichment analysis (GSEA) were performed using clusterProfiler R software.

Statistical analysis

All experiments were repeated three times independently. The biological triplicate results were presented as mean ± standard deviation using GraphPad Prism (ver. 6.01; GraphPad Software, Inc.). Data were analyzed by one-way ANOVA for comparisons. $^{*}P < 0.05$, $^{**}P < 0.01$, $^{***}P < 0.001$, ns: no significant.

Results

Construction and identification of MFN2-KD and MFN2-OE iPSCs

To demonstrate the function of *MFN2* in iPSCs, we constructed *MFN2*-KD and *MFN2*-OE iPSCs by the lentivirus-based system. In terms of cell morphology, *MFN2*-KD and *MFN2*-OE iPSCs showed little change with control iPSCs (Fig. 1A). Western blot and qRT-PCR were performed to detect the knockdown and overexpression efficiency of MFN2 (Fig. 1B). Immunofluorescence analysis showed the expression and distribution of MFN2 in control, *MFN2*-KD, and *MFN2*-OE iPSCs (Fig. 1C).

The effect of MFN2 on the three germ layer differentiation of iPSCs

To investigate the function of *MFN2* in the three germ layer differentiation of iPSCs, we conducted neural ectoderm, hematopoietic progenitor cell (mesoderm), and endoderm differentiation.

For neural ectoderm differentiation, *MFN2*-KD iPSCs demonstrated an increased expression level of neural ectoderm markers *PAX6* and *SOX1* (Fig. 2A). For mesoderm differentiation, *MFN2*-KD iPSCs showed an increased level of mesoderm markers *T* and *MESP1* (Fig. 2B) and CD34-positive cells (Fig. 2C, D). For endoderm differentiation, *MFN2*-KD iPSCs demonstrated an increased mRNA level of markers *SOX17* and *GATA4* (Fig. 2E). PSC differentiation is closely related to energy metabolism and *MFN2* can affect the way of cellular energy metabolism. Extracellular oxygen consumption assay showed that *MFN2* knockdown enhanced OXPHOS (oxidative phosphorylation) rates and marker expression levels of iPSCs (Supplementary Fig. S2).

The effect of MFN2 on the differentiation of iPSCs into MSCs

To further evaluate the role of *MFN2* in the differentiation of iPSCs into MSCs, we conducted a series of assays to assess the iPSC-MSC output efficiency of control, *MFN2*-KD, and *MFN2*-OE iPSCs. The main criteria for identifying MSCs are the expression of MSC surface markers and the capacity of trilineage differentiation (osteogenesis, adipogenesis, and chondrogenesis) [19].

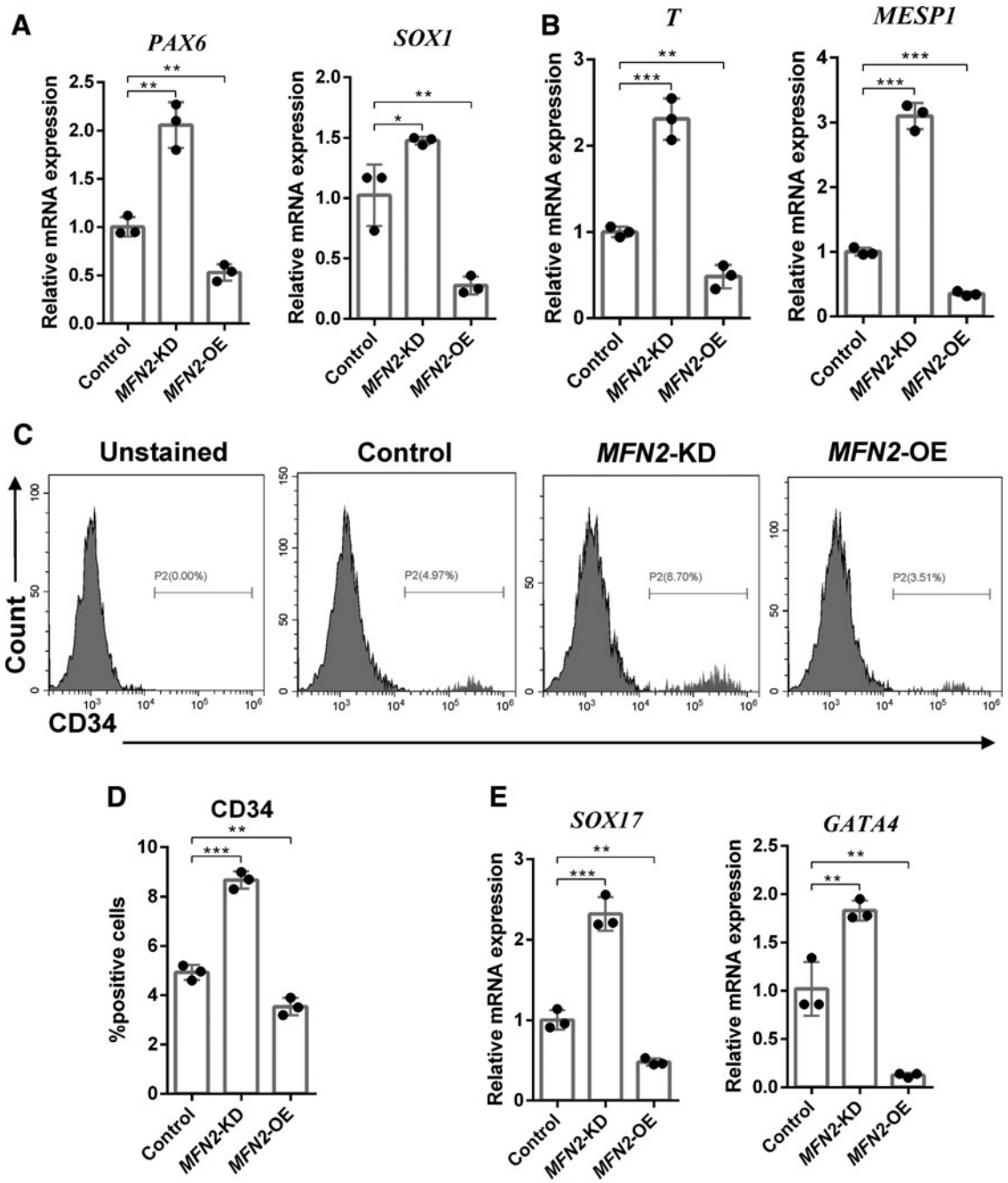

FIG. 2. The effect of *MFN2* on the three germ layer differentiation of iPSCs. **(A)** qRT-PCR analysis of neural ectoderm markers *PAX6* and *SOX1* in control, *MFN2*-KD, and *MFN2*-OE iPSCs. **(B)** qRT-PCR analysis of mesoderm markers *T* and *MESP1* in control, *MFN2*-KD, and *MFN2*-OE iPSCs. **(C, D)** Flow cytometry analysis of hematopoietic cell surface markers CD34 in control, *MFN2*-KD, and *MFN2*-OE iPSCs. **(E)** qRT-PCR analysis of endoderm markers *SOX17* and *GATA4* in control, *MFN2*-KD, and *MFN2*-OE iPSCs. *MFN2*-KD, *MFN2* knockdown. *MFN2*-OE, *MFN2* overexpressing. Data are expressed as mean ± SD, $*P < 0.05$, $**P < 0.01$, $***P < 0.001$.

MFN2-KD and *MFN2*-OE iPSC-MSCs showed little difference from control iPSC-MSCs, and both of them exhibited typical fibrous or polygonal morphology as MSCs (Fig. 3A). Flow cytometry demonstrated that the MSC surface markers CD73, CD90, and CD146 were highly expressed in the *MFN2*-KD group and expressed lower in the *MFN2*-OE group than the control (Fig. 3B). Hematopoietic cell surface markers CD34 and CD45 were hardly expressed in each group (Fig. 3D). Consistently, qRT-PCR results showed an increased expression level of MSC markers *NT5E* (CD73) and *ENG* (CD105) (Fig. 3C). In conclusion, the knockdown of *MFN2* promoted the differentiation of iPSCs into MSCs.

After 21 days of differentiation, the control, *MFN2*-KD, and *MFN2*-OE iPSC-MSCs were able to differentiate into the osteogenic (Fig. 4A), adipogenic (Fig. 4B), and

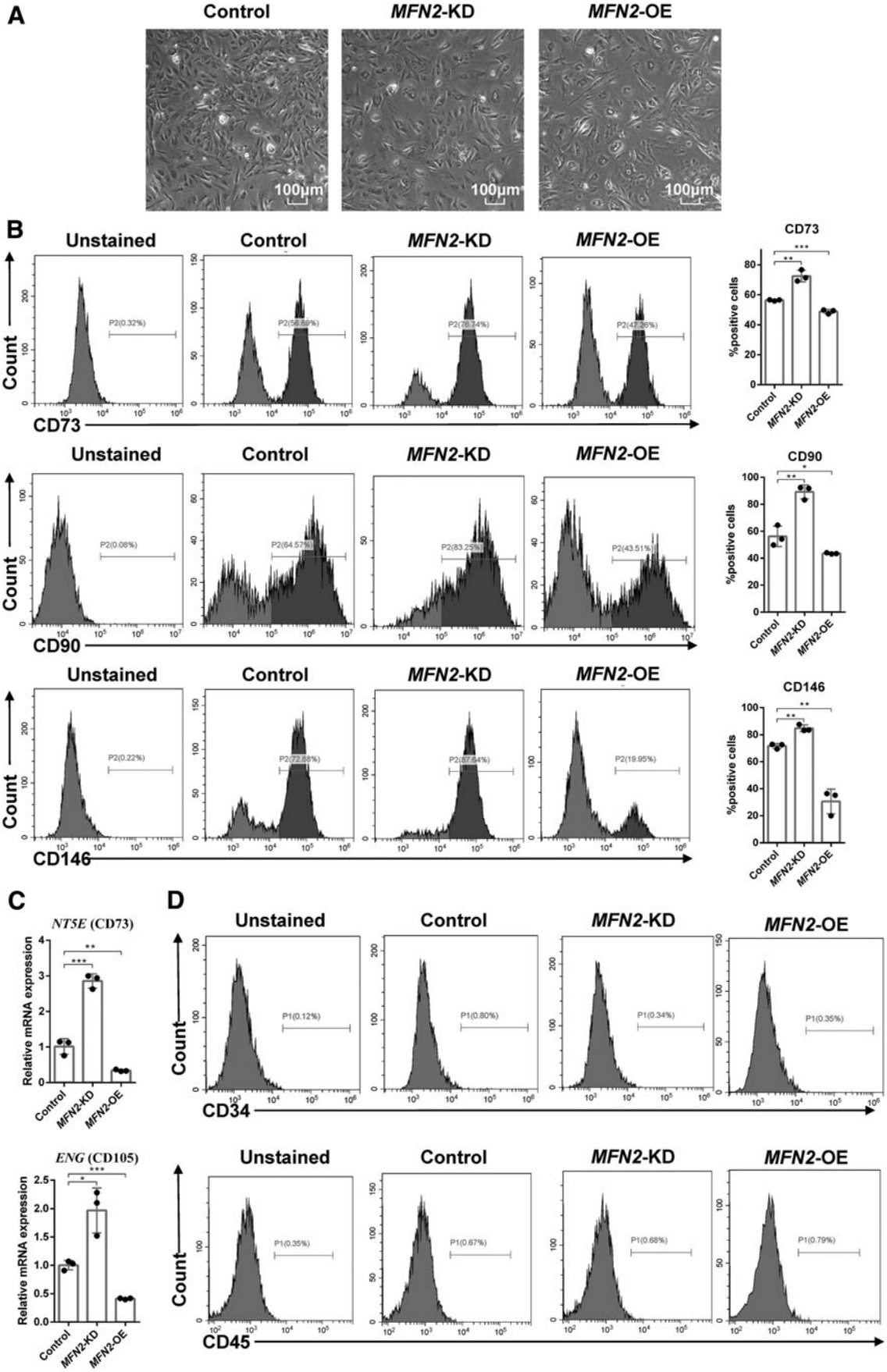

FIG. 3. The effect of *MFN2* on the differentiation of iPSCs into MSCs. **(A)** The morphology of control, *MFN2*-KD, and *MFN2*-OE iPSC-MSCs. Flow cytometry analysis of CD73, CD90, and CD146 **(B)**, qRT-PCR analysis of *NT5E* (CD73) and *ENG* (CD105) **(C)**, flow cytometry analysis of CD34 and CD45 **(D)** in control, *MFN2*-KD, and *MFN2*-OE iPSCs 8 days after differentiation into MSCs. *MFN2*-KD, *MFN2* knockdown. *MFN2*-OE, *MFN2* overexpressing. Data are expressed as mean ± SD, $*P < 0.05$, $**P < 0.01$, $***P < 0.001$. MSC, mesenchymal stem cell.

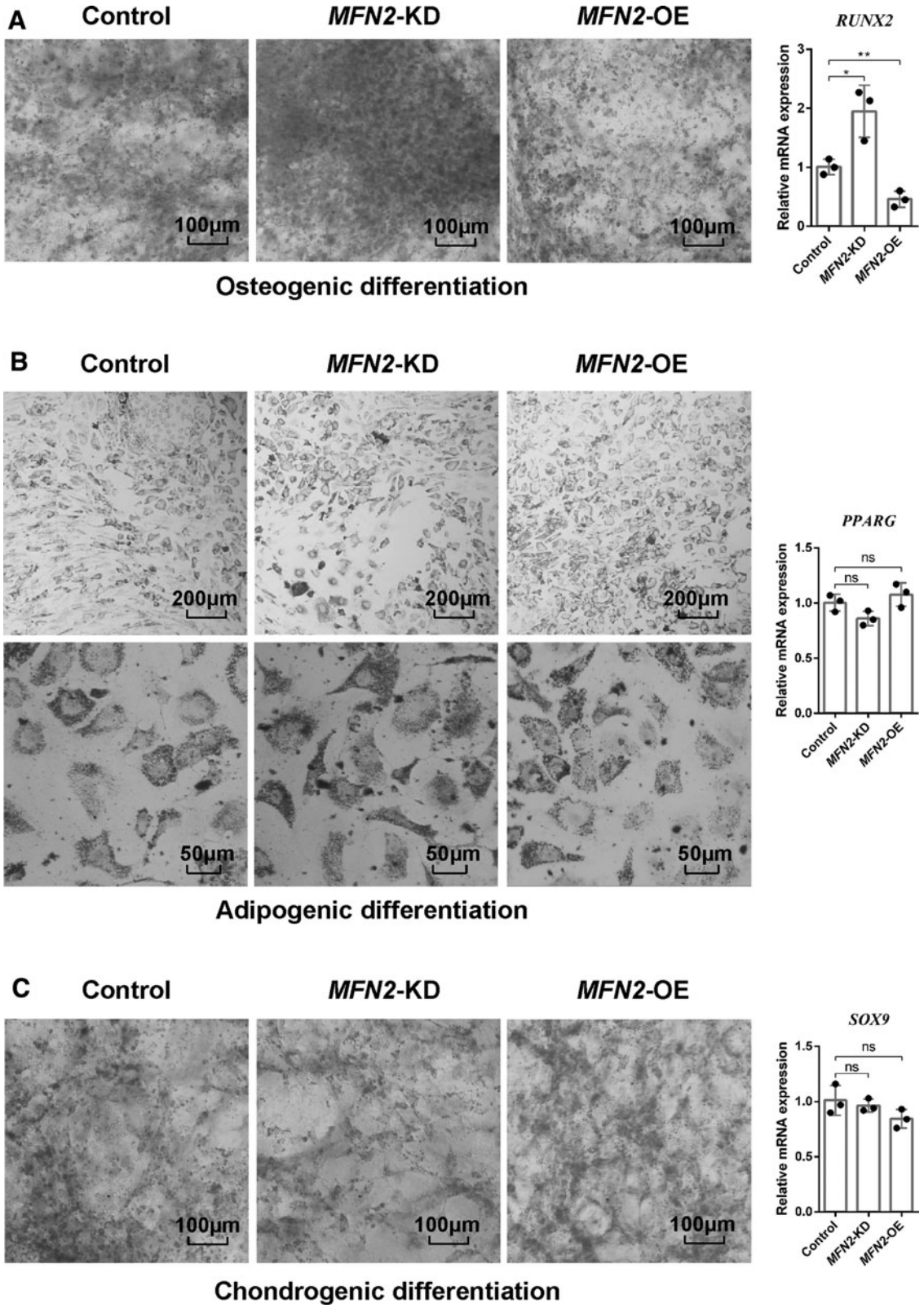

FIG. 4. Multilineage differentiation of iPSC-MSCs. Alizarin red staining and *RUNX2* expression **(A)** Oil Red O staining and *PPARG* expression **(B)** Alcian Blue staining and *SOX9* expression **(C)** of control, *MFN2*-KD, and *MFN2*-OE iPSC-MSCs after 21 days of differentiation. *MFN2*-KD, *MFN2* knockdown. *MFN2*-OE, *MFN2* overexpressing. ns, no significant. Data are expressed as mean ± SD, $*P < 0.05$, $**P < 0.01$.

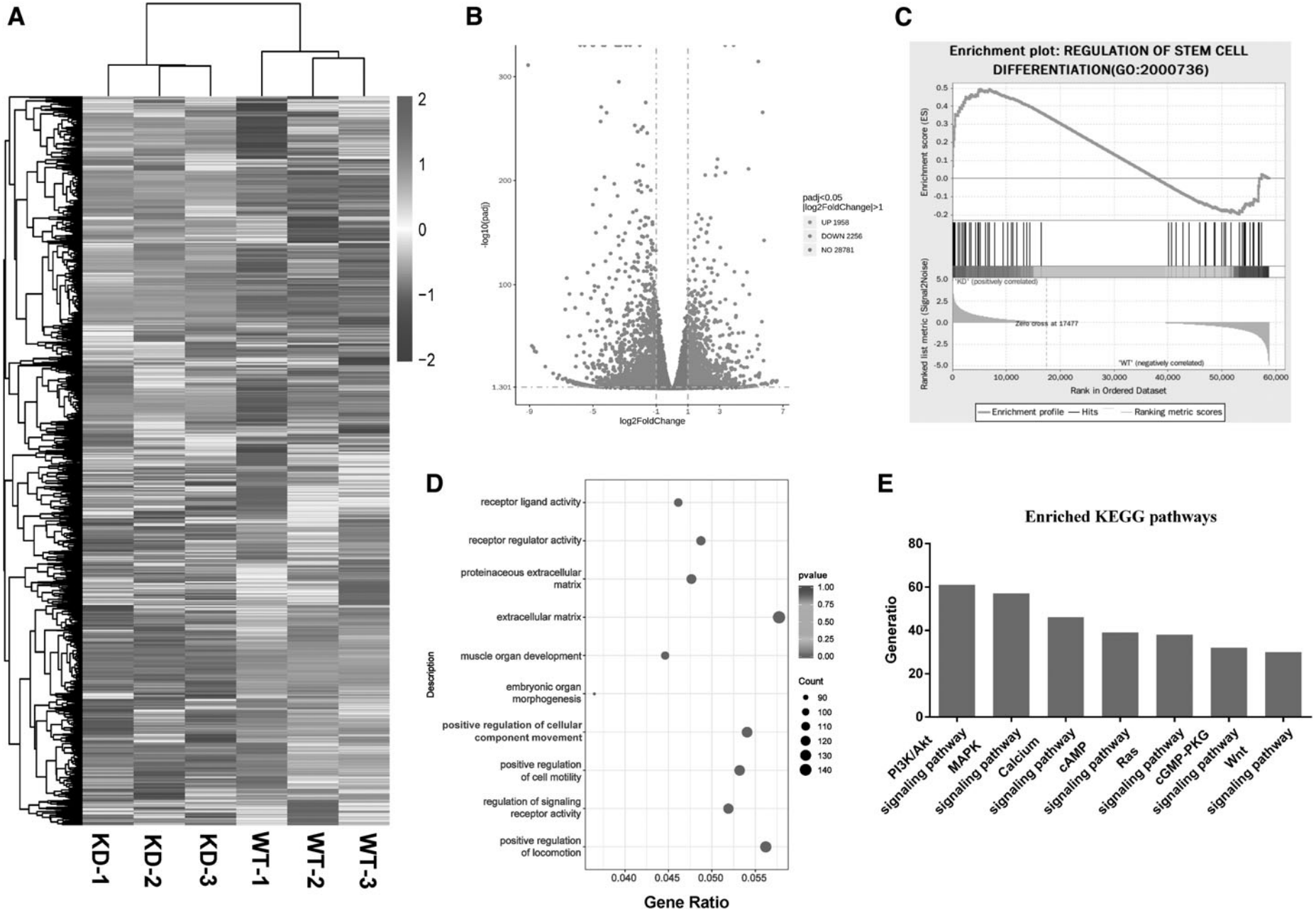

FIG. 5. Bioinformatics analysis of *MFN2*-KD iPSCs compared with control iPSCs. **(A)** Differentially expressed gene clustering heat map of control and *MFN2*-KD iPSCs. **(B)** The volcano map of differentially expressed genes. **(C)** GSEA plot showing *MFN2* expression in association with the regulation of stem cell differentiation. **(D)** The top 10 enriched terms of GO analysis. **(E)** Enriched KEGG pathways in *MFN2*-KD iPSCs. KD, *MFN2* knockdown. WT, wild-type (control iPSCs).

chondrogenic lineage (Fig. 4C). The results showed that there was no significant difference in adipogenic and chondrogenic differentiation capacity between control and *MFN2*-KD and *MFN2*-OE iPSC-MSCs. *MFN2*-KD iPSC-MSCs showed a stronger osteogenic differentiation capacity than control, while *MFN2*-OE was weaker (Fig. 4A and Supplementary Fig. S3).

Downregulating MFN2 promotes iPSC differentiation into MSCs by activating the PI3K/Akt signaling pathway

RNA-sequencing (RNA-seq) was conducted to obtain the differential gene expression profile of *MFN2*-KD and control iPSCs (Fig. 5A). There were 1,958 upregulated and 2,256 downregulated genes in *MFN2*-KD iPSCs compared with control iPSCs (Fig. 5B). The GSEA plot showed that *MFN2* expression was associated with the regulation of stem cell differentiation (Fig. 5C). The GO analysis showed that embryonic organ morphogenesis (GO:0048562) was in the top 10 enriched terms (Fig. 5D). Enrichment analysis of the KEGG pathway of differentially expressed genes found that the PI3K/Akt and Wnt signaling pathway was enriched (Fig. 5E).

Previous studies have shown that *MFN2* can participate in a series of cellular processes, such as cell proliferation, apoptosis, and differentiation by regulating the downstream PI3K/Akt signaling pathway [20]. Therefore, we evaluated the expression levels of pan AKT and phosphorylated AKT in control, *MFN2*-KD, and *MFN2*-OE iPSCs after eight days of culture in MSC induction medium. The *MFN2*-KD group showed an increase in PI3K/Akt signaling activation compared with the control and *MFN2*-OE groups (Fig. 6A). The PI3K/Akt signaling pathway was inhibited by 1 μM Akti-1/2 (S7776; Selleck) (Fig. 6B). Results showed that Akti-1/2 treatment of *MFN2*-KD iPSCs normalized the enhanced efficiency of differentiation into MSCs. Akt activator SC79 (5 μg/mL, S7863; Selleck) rescued the decreased efficiency of *MFN2*-OE iPSCs (Fig. 6C–E).

In conclusion, these data demonstrated that downregulating *MFN2* promoted iPSC differentiation into MSCs by activating the PI3K/Akt signaling pathway.

PI3K/Akt signaling pathway maintains Wnt/β-catenin activity via GSK-3β during the differentiation of iPSCs into MSCs

As mentioned before, the PI3K/Akt signaling pathway phosphorylates and inhibits GSK3β, thereby stabilizing β-catenin and promoting its transcription. Therefore, we evaluated the expression levels of pGSK-3β (phosphorylated GSK-3β) and β-catenin. The *MFN2*-KD group showed increases in pGSK-3β and β-catenin levels compared with the control group, which were normalized by Akti-1/2. The decreased levels of the *MFN2*-OE group were rescued by Akt activator SC79 (Fig. 7A, B). Wnt agonist 1 (5 μM, S8178; Selleck) simulates the role of the Wnt ligand as an activator of the Wnt signaling pathway. Wnt agonist 1 promoted the differentiation of the control iPSCs into MSCs, which were normalized by Akti-1/2. Wnt agonist 1 was not able to rescue the depressed capability of the *MFN2*-OE group due to the suppressed PI3K/Akt signaling pathway. (Fig. 7C–E).

In conclusion, PI3K/Akt signaling pathway maintained Wnt/β-catenin activity through GSK-3β during the differentiation of iPSCs into MSCs. *MFN2* knockdown promoted the differentiation of iPSCs into MSCs through the PI3K/Akt/GSK-3β/Wnt signaling pathway.

Discussion

Numerous kinds of cells have been utilized in periodontal tissue regeneration, but the quantity of these cells is limited, iPSC-MSCs are easier and infinitely obtainable [21]. Previous studies have shown that MSCs can be effectively differentiated from hPSCs under defined environments, factors, and stepwise protocols [22], but we still need a more time-saving method.

iPSCs are more inclined to differentiate back to their original lineage [23], which may be due to transcription factor-based reprogramming-derived iPSCs that have residual DNA methylation characteristics of the somatic tissue of their origin [6]. Interestingly, our previous studies reprogrammed human gingival fibroblasts to iPSCs [7], which were more effective in periodontal differentiation in vitro and in vivo [24]. Therefore, the MSCs derived from human gingival fibroblast-derived iPSCs in this study are expected to become efficient seed cells for periodontal regeneration.

Mitochondria are the principal location for energy production. The morphology of mitochondria changes to meet cellular energy needs and is maintained by the balance of fusion and fission. Mitochondrial dynamics also significantly affect stem cell function and fate [25].

As one of the key genes of mitochondrial fusion, *MFN2* can affect the way of cellular energy metabolism. Studies have shown that *MFN2* positively regulates oxidative phosphorylation (OXPHOS) [26]. Other studies have shown a negative effect of *MFN2* in OXPHOS [27]. Our results showed that *MFN2* knockdown enhanced OXPHOS level in iPSCs. Studies have shown that PSCs are not highly

FIG. 6. Downregulating *MFN2* promotes iPSC differentiation into MSCs by activating the PI3K/Akt signaling pathway. **(A)** Western blot analysis of pAKT and AKT in control, *MFN2*-KD, and *MFN2*-OE iPSCs eight days after differentiation into MSCs. **(B)** Western blot analysis of pAKT and AKT in control, *MFN2*-KD, and Akti-1/2-treated iPSCs eight days after differentiation into MSCs. **(C)** qRT-PCR analysis of *NT5E* (CD73) and *ENG* (CD105) in control, *MFN2*-KD, Akti-1/2-treated *MFN2*-KD iPSCs, *MFN2*-OE and SC79-treated *MFN2*-OE iPSCs eight days after differentiation into MSCs. **(D, E)** Flow cytometry analysis of CD73, CD90, and CD146 in control, *MFN2*-KD, Akti-1/2-treated *MFN2*-KD iPSCs, *MFN2*-OE, and SC79-treated *MFN2*-OE iPSCs eight days after differentiation into MSCs. *MFN2*-KD, *MFN2* knockdown. *MFN2*-OE, *MFN2* overexpressing. ns, no significant. Data are expressed as mean ± SD, $*P < 0.05$, $**P < 0.01$, $***P < 0.001$.

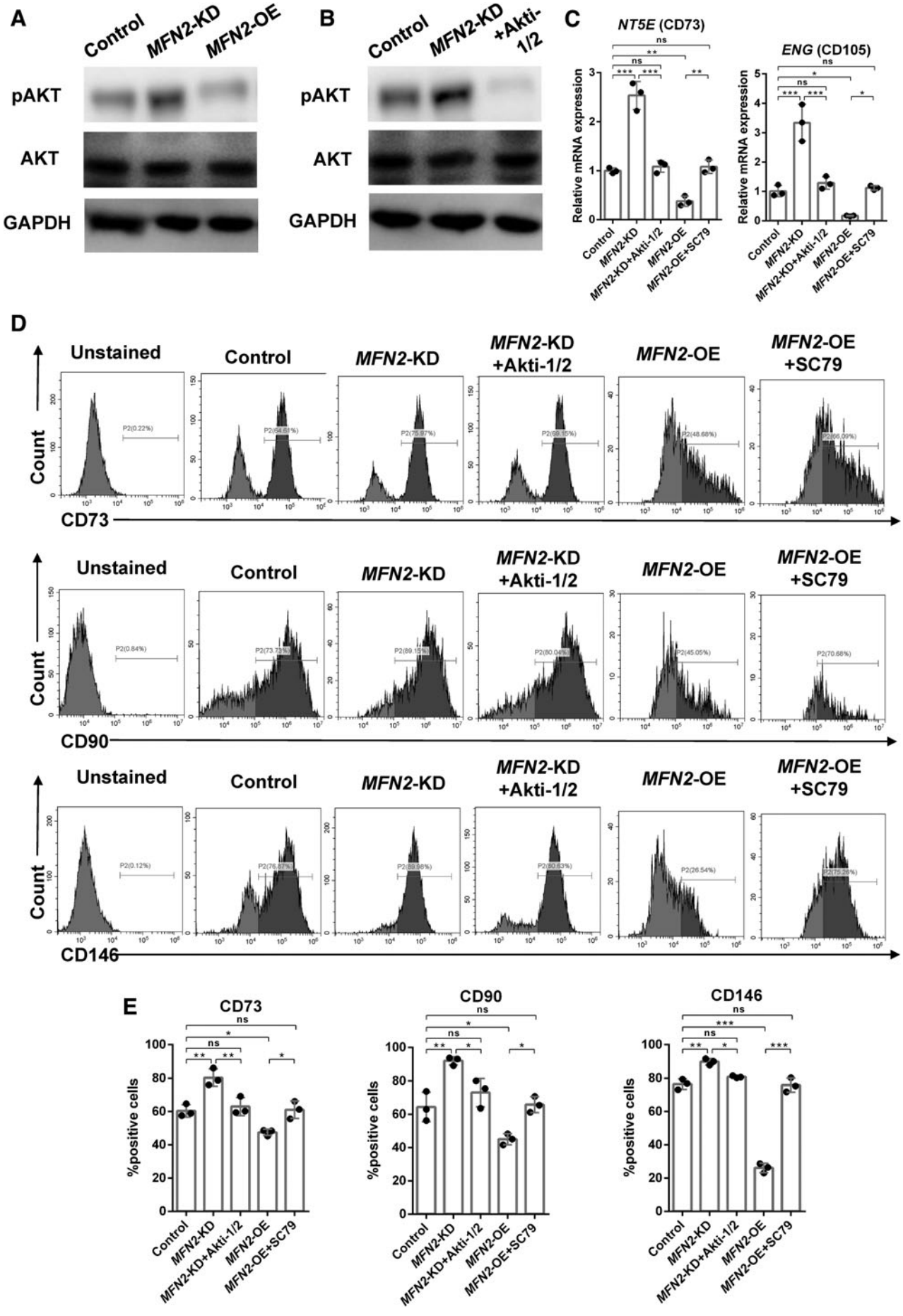

dependent on mitochondria for energy, while increased OXPHOS promotes PSC germ layer differentiation and loss of pluripotency [28]. Therefore, we deduced that *MFN2* knockdown may promote the three germ layer differentiation of iPSCs by enhancing OXPHOS. Further in-depth studies are needed to clarify the relationship among *MFN2*, germ layer differentiation, and energy metabolism.

The role of *MFN2* in the differentiation of PSCs has not yet been fully understood; therefore, controversial results exist. Downregulation of *MFN2* in inflammatory periodontal ligament stem cells promotes its osteogenic differentiation [29]. On the contrary, knocking out *MFN1*, *MFN2*, or *OPA1* in mouse ESCs inhibits the differentiation of ESCs into cardiomyocytes [30]. Double knockdown of *MFN1* and *MFN2* in iPSCs downregulates the gene expression of neural differentiation [31]. We demonstrated that knockdown of *MFN2* promoted the differentiation of iPSCs into MSCs, while overexpression of *MFN2* resulted in the opposite. The difference in the results of *MFN2* in PSC differentiation may be due to the differences in cell culture conditions, differentiation methods, and the mechanisms involved.

It has been reported that the PI3K/Akt signaling pathway is closely related to *MFN2*, and *MFN2* participates in a series of life processes such as cell proliferation and apoptosis by regulating the downstream PI3K/Akt signaling pathway [20]. *MFN2* inhibits the activation of mTORC2 and AKT through direct interaction by binding to its HR1 domain [32]. These studies demonstrate that *MFN2* can inhibit the PI3K/Akt signaling pathway, which is consistent with our results.

The role of the PI3K/Akt signaling pathway in PSCs is still controversial, it may play different roles in different types of differentiation. Some reports suggest that it maintains pluripotency [33]. Inhibition of PI3K/Akt/mTOR signaling can promote the endothelial differentiation of mouse PSC-derived endothelial-like progenitors [34]. Downregulating PI3K/Akt signaling effectively promotes mesendoderm and definitive endoderm of hESCs [35]. Inhibition of the PI3K/Akt pathway can increase the expression of hematopoietic genes of common marmoset ESCs [36].

Other reports suggest that it activates differentiation [37]. Extracellular IL-37 promotes osteogenic differentiation of MSCs through activation of the PI3K/Akt signaling pathway [38]. Matrix metalloproteinase-2 and melatonin significantly increase neural differentiation of iPSCs by activating the PI3K/Akt signaling pathway [39,40]. Erythropoietin treatment may stimulate the phosphorylation of ERK1/2 and AKT, which promotes the differentiation of mouse ESCs into definitive endoderm [41].

Similarly, our results showed that the inhibition of the PI3K/Akt signaling pathway in *MFN2*-KD iPSCs normalized the enhanced efficiency of differentiation into mesoderm-derived MSCs. This different effect may be due to the regulation of AKT by different complexes [42].

The AKT protein includes three isoforms with similar domains: AKT1 and AKT2 are widely expressed in all tissues, and AKT3 expression is limited to the brain and testis [43]. Studies have found that the coexpression of *AKT1* and *WNT11* may synergistically promote the survival and proliferation of MSCs and reduce apoptosis [44]. AKT1 maintains the complete development of the body, and due to its higher and wider expression pattern, it seems to play a more important role than other isoforms in the development process. AKT2 is related to insulin-regulated metabolic processes; AKT3 is involved in postnatal brain development and cell proliferation [45–47].

In our study, although both AKT1 and AKT2 were inhibited, it may be AKT1 that played a more critical role in the differentiation of iPSCs into MSCs. We will continue to study its specific mechanism and clarify its target in the future.

The PI3K/AKT/Gsk-3β signaling pathway participates in the regulation of many important biological processes [48]. Whether the Wnt/β-catenin and PI3K/Akt signaling pathways interact through the regulation of GSK-3β is still controversial. Previous studies have shown that the Wnt/β-catenin and PI3K/Akt signaling pathways are pharmacologically different [37]. Our study clarified that the PI3K/Akt signaling pathway maintained the Wnt/β-catenin pathway through the phosphorylation of GSK-3β during the iPSC differentiation into MSCs.

Our results showed that there was no significant difference in adipogenic and chondrogenic differentiation capacity between control and *MFN2*-KD and *MFN2*-OE iPSC-MSCs. The possible explanation is that *MFN2* does not affect adipogenic and chondrogenic differentiation. Studies have shown that increased expression of *MFN2* leads to a decrease in osteogenic differentiation of periodontal ligament stem cells owing to endoplasmic reticulum-mitochondria coupling [29]. *MFN2* conditional knockout female mice show an increased oxygen consumption, which enhanced cortical bone formation [49]. Similarly, our results demonstrated that *MFN2*-KD iPSC-MSCs had a stronger osteogenic differentiation capacity than control, which may be due to the above mechanism.

Further work in this area of research is required. We will identify the effect of *MFN2* on the energy utilization of iPSCs, as well as on the differentiation, immunomodulatory, and regeneration capacity of iPSC-MSCs in vivo in the periodontal defect model, which can result in a better understanding of the function of *MFN2* and serve the periodontal tissue regeneration.

FIG. 7. PI3K/Akt signaling pathway maintains Wnt/β-catenin activity through GSK-3β during the differentiation of iPSCs into MSCs. **(A, B)** Western blot analysis of pGSK-3β and β-catenin in control, *MFN2*-OE, *MFN2*-KD, SC79, and Akti-1/2-treated iPSCs eight days after differentiation into MSCs. **(C)** qRT-PCR analysis of *NT5E* (CD73) and *ENG* (CD105) in control, *MFN2*-OE, Wnt agonist 1, and Akti-1/2-treated iPSCs eight days after differentiation into MSCs. **(D, E)** Flow cytometry analysis of CD73, CD90, and CD146 in control, *MFN2*-OE, Wnt agonist 1, and Akti-1/2-treated iPSCs eight days after differentiation into MSCs. *MFN2*-KD, *MFN2* knockdown. *MFN2*-OE, *MFN2* overexpressing. ns, no significant. Data are expressed as mean ± SD, $^{**}P < 0.01$, $^{***}P < 0.001$.

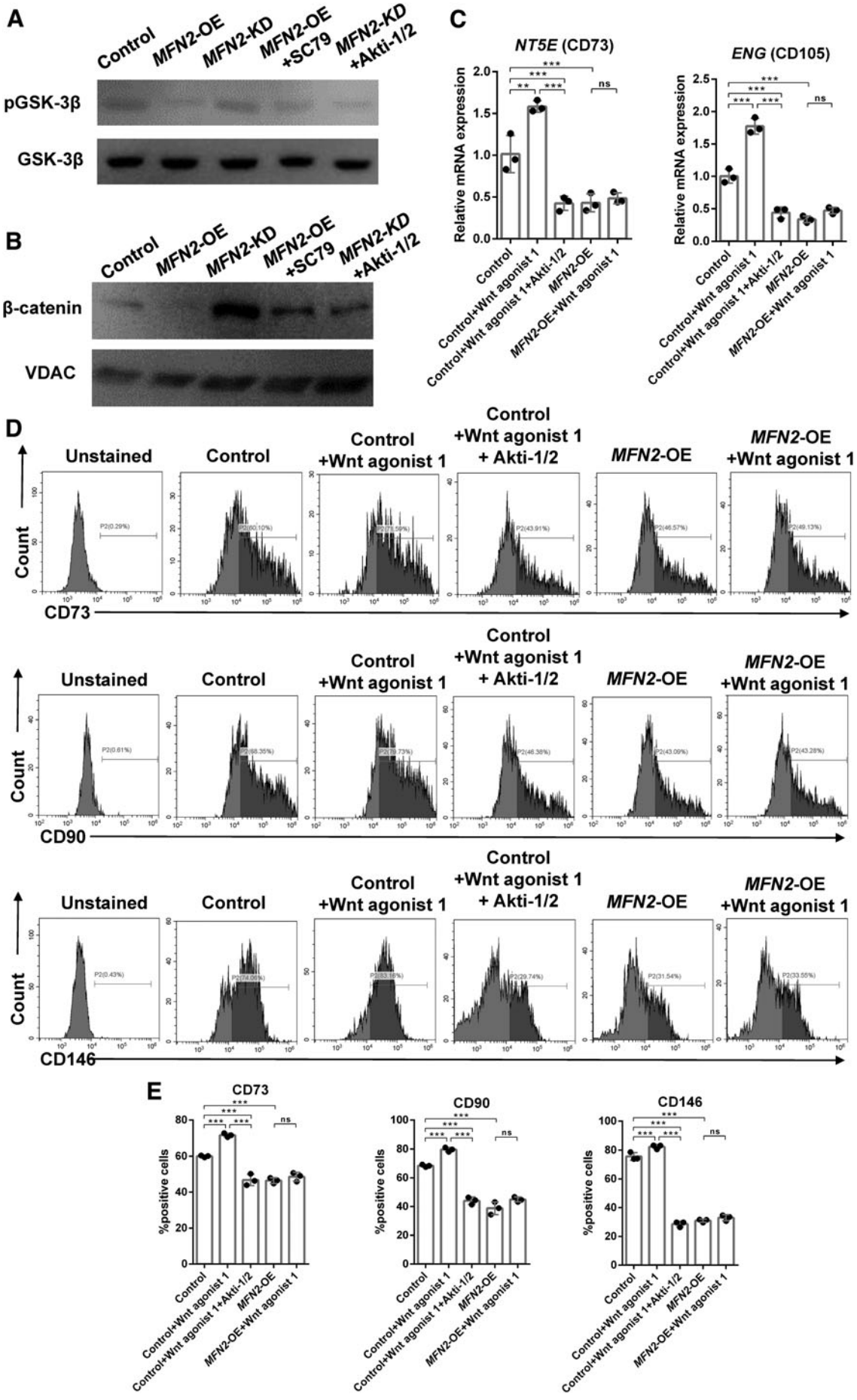

Author Disclosure Statement

No competing financial interests exist.

Funding information

This work was funded by the National Natural Science Foundation of China (grant numbers: 81870774, 31571517, 81800987) and the Beijing Municipal Natural Science Foundation (grant numbers: 7192091).

Data Statement

All data generated or analyzed during this study are included in this published article. The RNA-seq data have been uploaded to SRA (SRR14040003, SRR14040004, SRR14040005, SRR14040006, SRR14040007, SRR14040008).

Supplementary Material

Supplementary Figure S1
Supplementary Figure S2
Supplementary Figure S3

References

1. Yin X, P Li, Y Li, Y Cai, J Wen and Q Luan. (2017). Growth/differentiation factor-5 promotes in vitro/vivo periodontal specific differentiation of induced pluripotent stem cell-derived mesenchymal stem cells. Exp Ther Med 14:4111–4117.
2. Paccola MF, C Hochman-Mendez, J Morrissey, LC Sampaio and DA Taylor. (2019). Laminin as a potent substrate for Large-Scale expansion of human induced pluripotent stem cells in a closed cell expansion system. Stem Cells Int 2019:9704945.
3. Zakrzewski W, M Dobrzynski, M Szymonowicz and Z Rybak. (2019). Stem cells: past, present, and future. Stem Cell Res Ther 10:68.
4. Chow L, V Johnson, D Regan, W Wheat, S Webb, P Koch and S Dow. (2017). Safety and immune regulatory properties of canine induced pluripotent stem cell-derived mesenchymal stem cells. Stem Cell Res 25:221–232.
5. Polo JM, S Liu, ME Figueroa, W Kulalert, S Eminli, KY Tan, E Apostolou, M Stadtfeld, Y Li, et al. (2010). Cell type of origin influences the molecular and functional properties of mouse induced pluripotent stem cells. Nat Biotechnol 28:848–855.
6. Kim K, A Doi, B Wen, K Ng, R Zhao, P Cahan, J Kim, MJ Aryee, H Ji, et al. (2010). Epigenetic memory in induced pluripotent stem cells. Nature 467:285–290.
7. Yin X, Y Li, J Li, P Li, Y Liu, J Wen and Q Luan. (2016). Generation and periodontal differentiation of human gingival fibroblasts-derived integration-free induced pluripotent stem cells. Biochem Biophys Res Commun 473:726–732.
8. Sheyn D, S Ben-David, G Shapiro, S De Mel, M Bez, L Ornelas, A Sahabian, D Sareen, X Da, et al. (2016). Human induced pluripotent stem cells differentiate into functional mesenchymal stem cells and repair bone defects. Stem Cells Transl Med 5:1447–1460.
9. Meyer JN, TC Leuthner and AL Luz. (2017). Mitochondrial fusion, fission, and mitochondrial toxicity. Toxicology 391:42–53.
10. Rovira-Llopis S, C Banuls, N Diaz-Morales, A Hernandez-Mijares, M Rocha and VM Victor. (2017). Mitochondrial dynamics in type 2 diabetes: pathophysiological implications. Redox Biol 11:637–645.
11. Song M, K Mihara, Y Chen, L Scorrano and GN Dorn. (2015). Mitochondrial fission and fusion factors reciprocally orchestrate mitophagic culling in mouse hearts and cultured fibroblasts. Cell Metab 21:273–286.
12. Fang D, S Yan, Q Yu, D Chen and SS Yan. (2016). Mfn2 is required for mitochondrial development and synapse formation in human induced pluripotent stem Cells/hiPSC derived cortical neurons. Sci Rep 6:31462.
13. Chen W, Y Sun, Q Sun, J Zhang, M Jiang, C Chang, X Huang, C Wang, P Wang, et al. (2020). MFN2 plays a distinct role from MFN1 in regulating spermatogonial differentiation. Stem Cell Rep 14:803–817.
14. Xue R, X Zhu, L Jia, J Wu, J Yang, Y Zhu and Q Meng. (2019). Mitofusin2, a rising star in acute-on-chronic liver failure, triggers macroautophagy via the mTOR signalling pathway. J Cell Mol Med 23:7810–7818.
15. Hur EM and FQ Zhou. (2010). GSK3 signalling in neural development. Nat Rev Neurosci 11:539–551.
16. Gomez-Salinero JM, MM Lopez-Olaneta, P Ortiz-Sanchez, J Larrasa-Alonso, A Gatto, LE Felkin, P Barton, I Navarro-Lerida, DPM Angel, et al. (2016). The calcineurin variant CnAbeta1 controls mouse embryonic stem cell differentiation by directing mTORC2 membrane localization and activation. Cell Chem Biol 23:1372–1382.
17. Tian Y, ED Cohen and EE Morrisey. (2010). The importance of Wnt signaling in cardiovascular development. Pediatr Cardiol 31:342–348.
18. Yi S, X Huang, S Zhou, Y Zhou, MK Anderson, JC Zuniga-Pflucker, Q Luan and Y Li. (2020). E2A regulates neural ectoderm fate specification in human embryonic stem cells. Development 147:dev190298.
19. Zhou LL, W Liu, YM Wu, WL Sun, CE Dorfer and EK Fawzy. (2020). Oral mesenchymal Stem/Progenitor cells: the immunomodulatory masters. Stem Cells Int 2020:1327405.
20. Zhang D, C Ma, S Li, Y Ran, J Chen, P Lu, S Shi and D Zhu. (2012). Effect of Mitofusin 2 on smooth muscle cells proliferation in hypoxic pulmonary hypertension. Microvasc Res 84:286–296.
21. Hynes K, D Menicanin, J Han, V Marino, K Mrozik, S Gronthos and PM Bartold. (2013). Mesenchymal stem cells from iPS cells facilitate periodontal regeneration. J Dent Res 92:833–839.
22. Li E, Z Zhang, B Jiang, L Yan, JW Park and RH Xu. (2018). Generation of mesenchymal stem cells from human embryonic stem cells in a complete serum-free condition. Int J Biol Sci 14:1901–1909.
23. Bar-Nur O, HA Russ, S Efrat and N Benvenisty. (2011). Epigenetic memory and preferential lineage-specific differentiation in induced pluripotent stem cells derived from human pancreatic islet beta cells. Cell Stem Cell 9: 17–23.
24. Li J, X Yin and Q Luan. (2018). Comparative study of periodontal differentiation propensity of induced pluripotent stem cells from different tissue origins. J Periodontol 89:1230–1240.
25. Paliwal S, R Chaudhuri, A Agrawal and S Mohanty. (2018). Regenerative abilities of mesenchymal stem cells through mitochondrial transfer. J Biomed Sci 25:31.
26. Li T, J Han, L Jia, X Hu, L Chen and Y Wang. (2019). PKM2 coordinates glycolysis with mitochondrial fusion and oxidative phosphorylation. Protein Cell 10:583–594.
27. Yu M, ND Nguyen, Y Huang, D Lin, TN Fujimoto, JM Molkentine, A Deorukhkar, Y Kang, LF San, et al. (2019). Mitochondrial fusion exploits a therapeutic vulnerability of pancreatic cancer. JCI Insight 5:e126915.

28. Tsogtbaatar E, C Landin, K Minter-Dykhouse and C Folmes. (2020). Energy metabolism regulates stem cell pluripotency. Front Cell Dev Biol 8:87.
29. Zhai QM, B Li, ZW Wang, L Liu, Y Jin and F Jin. (2018). [Endoplasmic reticulum-mitochondrial contact regulates osteogenic differentiation of periodontal ligament stem cells via mitofusion 2 in inflammatory microenvironment]. Zhonghua Kou Qiang Yi Xue Za Zhi 53:453–458.
30. Kasahara A, S Cipolat, Y Chen, GN Dorn and L Scorrano. (2013). Mitochondrial fusion directs cardiomyocyte differentiation via calcineurin and Notch signaling. Science 342:734–737.
31. Yamada S, D Yamazaki and Y Kanda. (2018). 5-Fluorouracil inhibits neural differentiation via Mfn1/2 reduction in human induced pluripotent stem cells. J Toxicol Sci 43:727–734.
32. Xu K, G Chen, X Li, X Wu, Z Chang, J Xu, Y Zhu, P Yin, X Liang and L Dong. (2017). MFN2 suppresses cancer progression through inhibition of mTORC2/Akt signaling. Sci Rep 7:41718.
33. Watanabe S, H Umehara, K Murayama, M Okabe, T Kimura and T Nakano. (2006). Activation of Akt signaling is sufficient to maintain pluripotency in mouse and primate embryonic stem cells. Oncogene 25:2697–2707.
34. Que J, Q Lian, OR El, B Lim and SK Lim. (2007). PI3K/Akt/mTOR-mediated translational control regulates proliferation and differentiation of lineage-restricted RoSH stem cell lines. J Mol Signal 2:9.
35. McLean AB, KA D'Amour, KL Jones, M Krishnamoorthy, MJ Kulik, DM Reynolds, AM Sheppard, H Liu, Y Xu, EE Baetge and S Dalton. (2007). Activin a efficiently specifies definitive endoderm from human embryonic stem cells only when phosphatidylinositol 3-kinase signaling is suppressed. Stem Cells 25:29–38.
36. Nii T, T Marumoto, H Kohara, S Yamaguchi, H Kawano, E Sasaki, Y Kametani and K Tani. (2015). Improved hematopoietic differentiation of primate embryonic stem cells by inhibition of the PI3K-AKT pathway under defined conditions. Exp Hematol 43:901–911.
37. Naito AT, H Akazawa, H Takano, T Minamino, T Nagai, H Aburatani and I Komuro. (2005). Phosphatidylinositol 3-kinase-Akt pathway plays a critical role in early cardiomyogenesis by regulating canonical Wnt signaling. Circ Res 97:144–151.
38. Ye C, W Zhang, K Hang, M Chen, W Hou, J Chen, X Chen, E Chen, L Tang, et al. (2019). Extracellular IL-37 promotes osteogenic differentiation of human bone marrow mesenchymal stem cells via activation of the PI3K/AKT signaling pathway. Cell Death Dis 10:753.
39. Shu T, C Liu, M Pang, J Wang, B Liu, W Zhou, X Wang, T Wu, Q Wang and L Rong. (2018). Effects and mechanisms of matrix metalloproteinase2 on neural differentiation of induced pluripotent stem cells. Brain Res 1678:407–418.
40. Shu T, T Wu, M Pang, C Liu, X Wang, J Wang, B Liu and L Rong. (2016). Effects and mechanisms of melatonin on neural differentiation of induced pluripotent stem cells. Biochem Biophys Res Commun 474:566–571.
41. Kaitsuka T, K Kobayashi, W Otsuka, T Kubo, F Hakim, FY Wei, N Shiraki, S Kume and K Tomizawa. (2017). Erythropoietin facilitates definitive endodermal differentiation of mouse embryonic stem cells via activation of ERK signaling. Am J Physiol Cell Physiol 312:C573–C582.
42. Guertin DA, DM Stevens, CC Thoreen, AA Burds, NY Kalaany, J Moffat, M Brown, KJ Fitzgerald and DM Sabatini. (2006). Ablation in mice of the mTORC components raptor, rictor, or mLST8 reveals that mTORC2 is required for signaling to Akt-FOXO and PKCalpha, but not S6K1. Dev Cell 11:859–871.
43. Cohen MJ. (2013). The AKT genes and their roles in various disorders. Am J Med Genet 161A:2931–2937.
44. Chen B, X Chen, C Liu, J Li, F Liu and Y Huang. (2018). Co-expression of Akt1 and Wnt11 promotes the proliferation and cardiac differentiation of mesenchymal stem cells and attenuates hypoxia/reoxygenation-induced cardiomyocyte apoptosis. Biomed Pharmacother 108:508–514.
45. Tang Y, Z Jiang, Y Luo, X Zhao, L Wang, C Norris and XC Tian. (2014). Differential effects of Akt isoforms on somatic cell reprogramming. J Cell Sci 127:3998–4008.
46. Hinz N and M Jucker. (2019). Distinct functions of AKT isoforms in breast cancer: a comprehensive review. Cell Commun Signal 17:154.
47. Yang ZZ, O Tschopp, N Di-Poi, E Bruder, A Baudry, B Dummler, W Wahli and BA Hemmings. (2005). Dosage-dependent effects of Akt1/protein kinase Balpha (PKBalpha) and Akt3/PKBgamma on thymus, skin, and cardiovascular and nervous system development in mice. Mol Cell Biol 25:10407–10418.
48. Tang J, MF Qing, M Li and Z Gao. (2020). Dexamethasone inhibits BMP7-induced osteogenic differentiation in rat dental follicle cells via the PI3K/AKT/GSK-3beta/beta-catenin pathway. Int J Med Sci 17:2663–2672.
49. Zarei A, A Ballard, L Cox, P Bayguinov, T Harris, JL Davis, P Roper, J Fitzpatrick, R Faccio and DJ Veis. (2021). Osteolineage depletion of mitofusin2 enhances cortical bone formation in female mice. Bone 148:115941.

Address correspondence to:
Dr. Yang Li
Department of Cell Biology
School of Basic Medical Sciences
Peking University Stem Cell Research Center
Peking University
Beijing 100191
People's Republic of China

E-mail: liyang@bjmu.edu.cn

Dr. Qingxian Luan
Department of Periodontology
Peking University School and Hospital of Stomatology
National Center of Stomatology
National Clinical Research Center for Oral Diseases
National Engineering Laboratory for Digital and Material Technology of Stomatology
Beijing Key Laboratory of Digital Stomatology
Research Center of Engineering and Technology for Computerized Dentistry Ministry of Health
NMPA Key Laboratory for Dental Materials
No.22, Zhongguancun South Avenue, Haidian District
Beijing 100081
People's Republic of China

E-mail: kqluanqx@126.com

Received for publication November 23, 2021
Accepted after revision January 25, 2022
Prepublished on Liebert Instant Online January 28, 2022